The Sailor-diagram. An extension of the Taylor diagram to two-dimensional variables for verification of model data

J. Sáenz, S. Carreno-Madinabeitia, G. Esnaola, S. J. González-Rojí, G. Ibarra-Berastegi, and A. Ulazia

EGU General Assembly 2020, May, 8th.

University of the Basque Country, UPV/EHU, TECNALIA, Basque Research and Technology Alliance (BRTA), Oeschger Centre for Climate Change Research, University of Bern

Introduction

Abstract.
We propose a diagram for verification of 2D vector fields (currents, vertically integrated moisture transport . . .):

- It visually presents the bias and the variance fractions of every vector field
- It conveys visual information on the relative rotation of vector fields
- It is based on the PCA-based decomposition of the 2D vector data:
  - Full rank for realistic vector fields, 2x2 covariance matrix
  - Exact value of RMSE assessed
  - Additional error statistics in our R implementation
  - Publicly available in CRAN as package SailoR
- It can also be used for spatial fields and ensemble forecast systems

The success of the Taylor diagram

- The paper describing the Taylor diagram has been cited over 2700 times since 2001.
- The success can be explained because the diagram:
    - is an efficient (fast, visual) tool to evaluate models
    - incorporates different (RMSE, variance, correlation coefficient) quality indicators
    - is flexible and can be applied to:
        - Spatial patterns
        - Time series
        - Ensembles

Taylor diagram and 2D vector data (wind, current. . .)

Different results for zonal/meridional components.

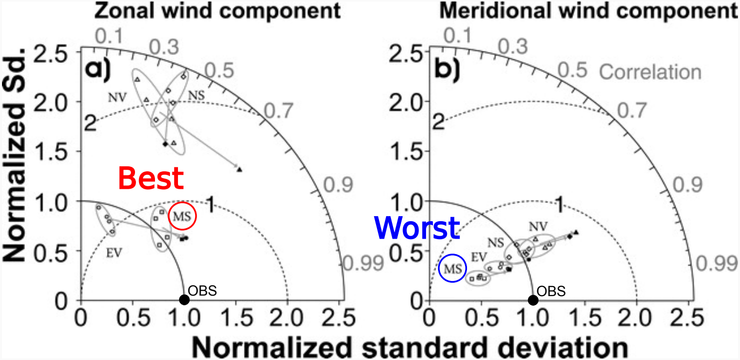

Figure 1: Zonal/Meridional switch

Figure 6 from Jiménez et al. (2020)

Use of magnitude is an alternative option

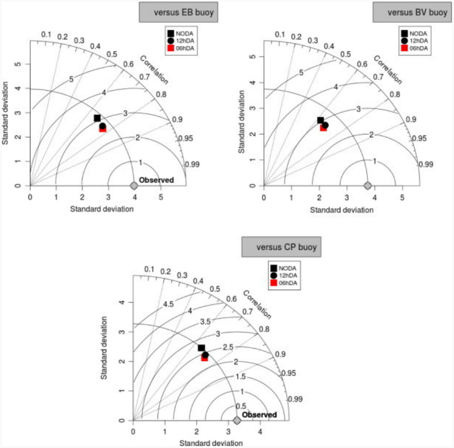

Figure 2: Magnitude of wind

Figure 4 from Ulazia et al., 2016, but directional information is lost.

Mean of zonal and meridional Taylor diagrams

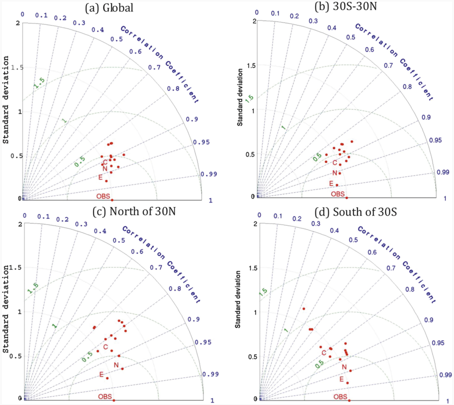

Figure 3: Mean of Taylor diagrams for zonal and meridional components of wind-stress

Figure 9 from Lee et al., 2013. Again, directional information is lost.

Proposed solution: The Sailor Diagram

Playing Carroll:

Taylor -> **Sailor**. Sailors need to measure currents, winds... 2D vectors.

Basis for a proposal

- There is no uniquely accepted version of a 2D correlation coefficient.
- We want to keep a diagnosis of the quality of directionality.
- We, therefore, forget the graphical setup of the Taylor diagram, but keep the idea of a fast visual diagnostic.
- Results, however, will be exact. 2D MSE error between observations U ($N \times 2$ matrix) and model simulation V ($N \times 2$ matrix):

$$\Delta_{uv}^2 = \frac{1}{N} (V - U)^T (V - U) \tag{1}$$

Playing with synthetic data

We consider as observations a one-year long (2017) dataset (*Ref*) of hourly wind (zonal and meridional components) from ERA5 reanalysis at the point 38°N and -124°W, near Los Angeles. The **principal axes** (no lost variance in 2D) of the data are shown.

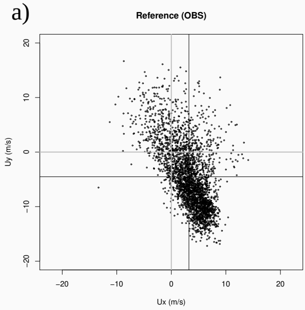

Figure 4: Scatterplot of zonal (X) and meridional components of wind in *Ref*

Playing with synthetic data (Cont.)

- Observational dataset *Ref*
- Synthetic *MOD1* added **constant bias**.
- Synthetic dataset *MOD2*: **30° counterclockwise rotation**.

Scatterplots and principal components (ellipses) are shown below.

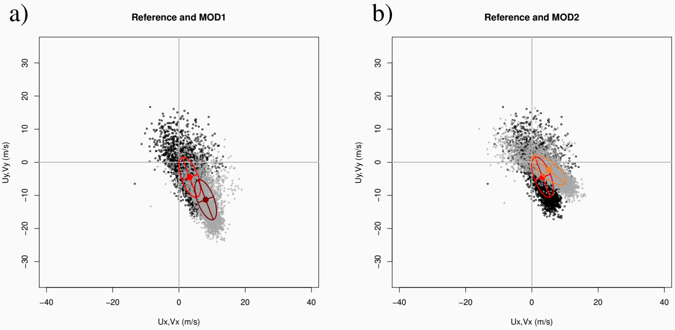

Figure 5: Scatterplots for *MOD1* and *MOD2* aginst *Ref*

Playing with synthetic data (Cont.)

- Observational dataset *Ref*
- Synthetic *MOD3* **random resampling** on top of *Ref*.
- Synthetic dataset *MOD4*: **multiplied by two**.

Scatterplots and principal components are shown below.

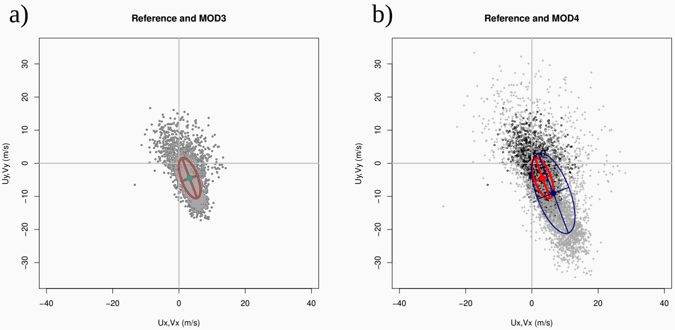

Figure 6: *MOD3* and *MOD4* against *Ref*

Playing with synthetic data (Cont.)

Dataset	Bias	Rotation	R^2	Var. Fraction
MOD1	$\neq 0$	0	2	1
MOD2	$\neq 0$	30°	2	1
MOD3	0	0	≈ 0	1
MOD4	$\neq 0$	0	2	4

For the squared of the correlation coefficient R^2, the definition by (Crosby et al., 1993) (perfect 2D correlation if $R^2 = 2$) is used.

Crosby, et al., 1993. A proposed definition for vector correlation in Geophysics: Theory and Application, Journal of Atmos. and Oceanic Technol., 10, 355–367.

Mathematical main steps

MSE obtained from Δ^2_{uv} through its Frobenius norm

$$\varepsilon^2 = ||\Delta^2_{uv}||_F. \tag{2}$$

Tool: projection onto EOFs. Full rank covariance!

$$S_u = \frac{1}{N}\left(U-\bar{U}\right)^T\left(U-\bar{U}\right) = \begin{pmatrix} S_{xx} & S_{xy} \\ S_{xy} & S_{yy} \end{pmatrix} \tag{3}$$

For 2D geophysical flows: $\texttt{rank}(S) = 2$. No variance lost using 2 EOFs.

$$U = \bar{U} + P_u^* \Sigma_u E_u^T = \bar{U} + P_u E_u^T \tag{4}$$

Model V projected onto U's EOFs (Full rank $\Rightarrow N_{eofs} = 2$)

V projected onto U observational EOFs using rotation matrix R_{vu}:

$$V = \bar{V} + P_v E_u^T R_{vu}^T \tag{5}$$

The ellipses defined by the principal components

The expression of the data in terms of principal components leads to this quadratic form (ellipses).

$$||P_u^* P_u^{*T}||_F = || \left(U - \bar{U}\right) E_u \Sigma_u^{-2} E_u^T \left(U - \bar{U}\right)^T ||_F = 1. \qquad (6)$$

The eccentricity of every ellipse is related to the variance of the corresponding semi-major and semi-minor axes (fraction of variance corresponding to each PC):

$$\varepsilon_u = \sqrt{1 - \frac{\sigma_{2u}^2}{\sigma_{1u}^2}} \qquad (7)$$

Error matrix:

$$\Delta^2_{uv} = \frac{1}{N} B^2_{uv} + \frac{1}{N} D_{uv} \tag{8}$$

Bias:

$$B^2_{uv} = \left(\bar{V} - \bar{U}\right)^T \left(\bar{V} - \bar{U}\right) \tag{9}$$

The errors due to directionality are expressed using EOFs from U (E_u), the rotation matrix R_{vu}, the standard deviations of PCs (Σ_u for observations and Σ_v for model) and the covariances of PCs corresponding to model and observations Γ_{vu}:

$$D_{uv} = E_u \Sigma_u^2 E_u^T + R_{vu} E_u \Sigma_v^2 E_u^T R_{vu}^T - \left(E_u \Gamma_{vu} E_u^T R_{vu}^T + R_{vu} E_u \Gamma_{vu}^T E_u^T\right) \tag{10}$$

The Sailor diagram graphically represents the bias $\bar{V} - \bar{U}$, the EOFs E_u and E_v, their eigenvalues λ_{ui} and λ_{vi} ($i = 1, 2$) and the rotation R_{vu}.

Resulting Sailor diagram for synthetic data

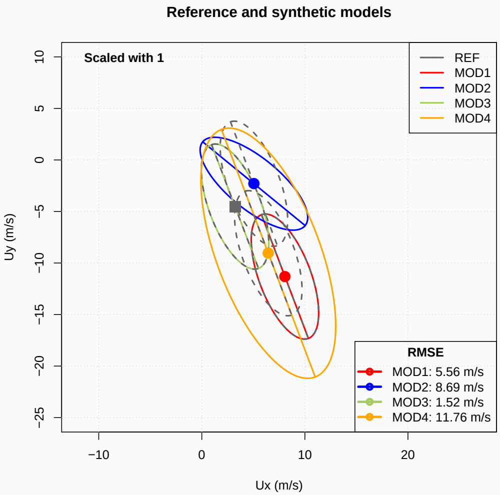

Figure 7: Diagram showing the means and ellipses (exact RMSE in the legend).

Sample of additional diagnostics provided in our package

- R^2 computed from CCA (Crossby et al., 1993)
- ε (eccentricity of the ellipses)
- Congruence coefficients of EOFs (degeneracy of eigenvalues)

$$g_{ii} = |\mathbf{e}_{ui} \cdot \mathbf{e}_{vi}| \tag{11}$$

- Relative rotation of axes (from R_{vu})
- Variances of zonal/meridional axes
- Variances of principal axes

Let's see them at work with the synthetic datasets.

Identifying the (known) errors in our synthetic datasets

Model	σ^2	$\sum_i \sigma_i^2$	θ_u	θ_v	θ_{vu}	R^2	$\lvert\texttt{bias}\rvert$	RMSE	ε	g_{11}
Ref	47.56	47.56	1.93			2.00	0.00	0.00	0.92	1.00
MOD1	47.56	47.56		1.93	0.00	2.00	8.34	5.56	0.92	1.00
MOD2	47.56	47.56		2.46	0.52	2.00	2.88	8.69	0.92	0.87
MOD3	47.56	47.56		-1.21	0.72	0.00	0.00	1.52	0.92	1.00
MOD4	190.24	190.24		1.93	0.00	2.00	5.56	11.76	0.92	1.00

Figure 8: Table of (some) diagnostics for synthetic models

- Bias in MOD1 ✔
- Rotation in MOD2 ✔
- Lack of correlation and no rotation in MOD3 ✔
- Change in variances ($\sigma_v^2 = \sigma_u^2 \times 2^2$) in MOD4 ✔

Results with real data and further degrees of freedom

1. **Scale factor to improve readability. Same plot, different scale.**

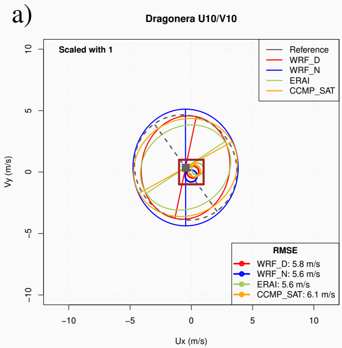

Figure 9: Application to wind data in a buoy (Dragonera)

Improves the visibility of the **bias**, distance from each model's average to the observational grey square

1. Scale factor. 2. Ellipses centered on top of observational mean.

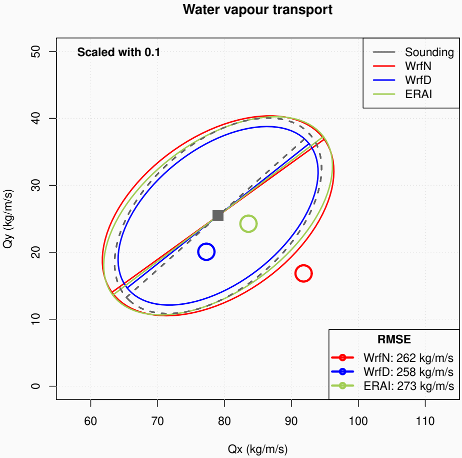

Figure 10: Vertically integrated moisture transports.

Ellipses share same center. Improves the perception of rotation and axes.

Application to time-averages over a Hemisphere.

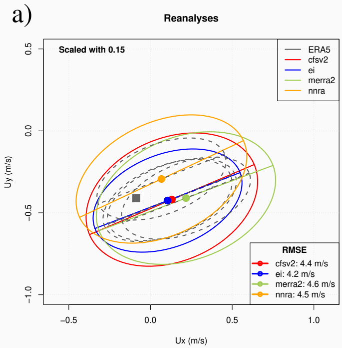

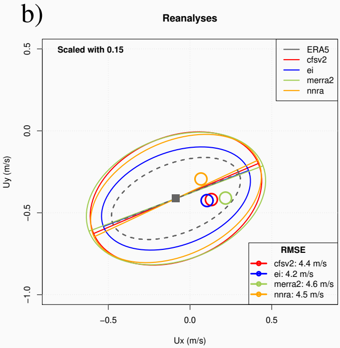

Figure 11: Multi-year January average of surface wind over NH

PCA is in this case applied in S-mode ➔(Richman, 1986)

Application to ensembles of models.

- Case 1. All realizations of a model joined together.
- Case 2. Every realization taken as an independent run.

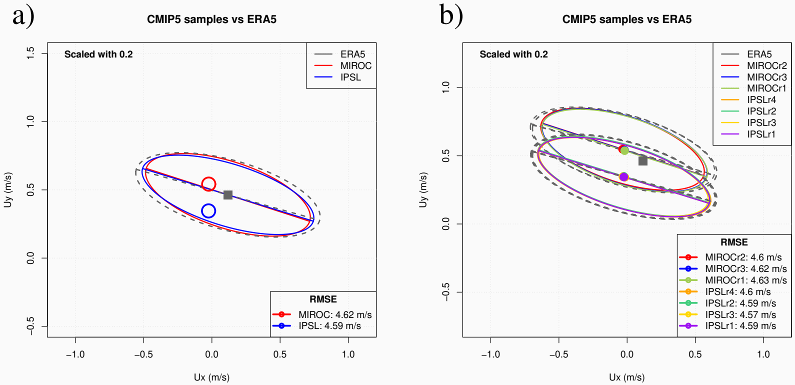

Figure 12: Southern Hemisphere from ERA5 and CMIP5 models

What about degeneracy of eigenvectors?

if $\varepsilon \approx 0$, the rotation angle can not be trusted but RMSE is still exact, since it does not depend on the degeneracy.

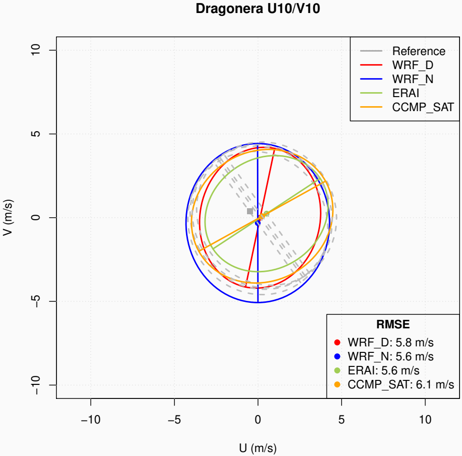

Figure 13: Both semiaxes are similar but RMSE is exact

Conclusions

- A diagram is presented which allows a fast visual comparison of simulations of 2D vector fields with observations.
- The diagram is constructed by expanding the squared error in a bias and a directional component.
- The directional component is assessed by means of the EOFs of the 2D distribution of wind/current.
- It can be applied to wind, current, vertically integrated moisture transport and any other 2D vector quantity.
- The diagram can be complemented with additional diagnostics such as the eccentricity of the ellipses, the congruence coefficients or the canonical correlations, parameters provided by our package.
- The diagram allows to identify errors in the bias, the orientation of the main directions of the vector datasets or their relative variances.
- The mathematical development is exact and the use of the RMSE error in the diagrams allows an exact comparison of the overall error.

R package publicly available

SailoR: An Extension of the Taylor Diagram to Two-Dimensional Vector Data

A new diagram for the verification of vector variables (wind, current, etc) generated by multiple models against a set of observations is presented in this package. It has been designed as a generalization of the Taylor diagram to two dimensional quantities. It is based on the analysis of the two-dimensional structure of the mean squared error matrix between model and observations. The matrix is divided into the part corresponding to the relative rotation and the bias of the empirical orthogonal functions of the data. The full set of diagnostics produced by the analysis of the errors between model and observational vector datasets comprises the errors in the means, the analysis of the total variance of both datasets, the rotation matrix corresponding to the principal components in observation and model, the angle of rotation of model-derived empirical orthogonal functions respect to the ones from observations, the standard deviation of model and observations, the root mean squared error between both datasets and the squared two-dimensional correlation coefficient. See the output of function UVError() in this package.

Version:	1.0
Depends:	R ($\geq$ 3.5.0)
Published:	2019-10-11
Author:	Jon Sáenz [aut, cph], Sheila Carreno-Madinabeitia [aut, cph], Santos J. González-Rojí [aut, cre, cph], Ganix Esnaola [ctb, cph], Gabriel Ibarra-Berastegi [ctb, cph], Alain Ulazia [ctb, cph]
Maintainer:	Santos J. González-Rojí <santosjose.gonzalez at ehu.eus>
License:	GPL-3
NeedsCompilation:	no
CRAN checks:	SailoR results

Downloads:

Reference manual:	SailoR.pdf
Package source:	SailoR_1.0.tar.gz
Windows binaries:	r-devel: SailoR_1.0.zip, r-devel-gcc8: SailoR_1.0.zip, r-release: SailoR_1.0.zip, r-oldrel: SailoR_1.0.zip
OS X binaries:	r-release: SailoR_1.0.tgz, r-oldrel: SailoR_1.0.tgz

Linking:

Please use the canonical form https://CRAN.R-project.org/package=SailoR to link to this page.

Figure 14: SailoR R package

Available from CRAN

Paper under discussion in Geoscientific Model Development

Submitted as: methods for assessment of models 19 Nov 2019

The Sailor diagram. An extension of Taylor's diagram to two-dimensional vector data

Review status

A revised version of this preprint is currently under review for the journal GMD.

Jon Sáenz[1,2], Sheila Carreno-Madinabeitia[3], Ganix Esnaola[4,2], Santos J. González-Rojí[5,6], Gabriel Ibarra-Berastegi[7,2], and Alain Ulazia[8]

[1]Dept. Applied Physics II, Universidad del País Vasco/Euskal Herriko Unibertsitatea (UPV/EHU), Barrio Sarriena s./n., 48940-Leioa, Spain
[2]Joint Research Unit BEGIK, Instituto Español de Oceanografía (IEO)-Universidad del País Vasco/Euskal HerrikoUnibertsitatea (UPV/EHU), Plentziako Itsas Estazioa, Areatza Pasealekua, 48620-Plentzia, Spain
[3]TECNALIA, Parque Tecnológico de Álava, Albert Einstein 28, 01510 Vitoria-Gasteiz, Spain
[4]Nuclear Engineering and Fluid Mechanics Dept., Gipuzkoako Ingeniaritza Eskola, Europa Plaza 1, 20018-Donostia, Spain
[5]Oeschger Centre for Climate Change Research, University of Bern, 3010 Bern, Switzerland
[6]Climate and Environmental Physics, University of Bern, 3010 Bern, Switzerland
[7]Nuclear Engineering and Fluid Mechanics Dept., Escuela de Ingeniería de Bilbao, Plaza Ingeniero Torres Quevedo 1, 48013-Bilbao, Spain
[8]Nuclear Engineering and Fluid Mechanics Dept., Gipuzkoako Ingeniaritza Eskola, Otaola etorbidea 29, 20600-Eibar, Spain

Received: 11 Oct 2019 – Accepted for review: 15 Nov 2019 – Discussion started: 19 Nov 2019

DOI: https://doi.org/10.5194/gmd-2019-289

Full documentation of the methodology in this paper (under review now)